JOURNAL OF VIROLOGY, Aug. 2008, p. 7475–7482 Vol. 82, No. 15
0022-538X/08/$08.00+0 doi:10.1128/JVI.02193-07

Suppression of Astrovirus Replication by an ERK1/2 Inhibitor▽

Lindsey A. Moser and Stacey Schultz-Cherry*

Department of Medical Microbiology and Immunology, University of Wisconsin—Madison, Madison, Wisconsin 53706

Received 5 October 2007/Accepted 19 May 2008

Human astroviruses are nonenveloped, positive-sense single-strand RNA viruses associated with self-limiting diarrhea. Although they are recognized as a leading cause of disease in young children, the cellular factors involved in astrovirus replication are not well defined. The extracellular signal-regulated kinase (ERK) pathway has been shown to regulate many viral infections, but its role during astrovirus infection is unknown. In this report, we show that astrovirus activates ERK1/2 early in infection independently of replication. Inhibition of ERK activation with U0126, a specific ERK inhibitor, significantly reduced viral production. Investigations into the mechanism of ERK1/2 regulation revealed that all steps of the viral life cycle, including early and late protein expression as well as subgenomic and genomic RNA transcription, were diminished during U0126 treatment of monolayers. These data support a role for ERK1/2 in a postattachment step, although the precise mechanism remains under investigation.

Human astroviruses (HAstVs) are small enteric viruses associated with diarrhea, primarily in young children, the elderly, and the immunocompromised. To date, eight serotypes, which have been named HAstV-1 to HAstV-8 based on genotypic and immunological distinctions, have been identified. HAstVs possess a positive-sense, single-stranded RNA genome of approximately 6.8 kb. The genome is comprised of three open reading frames (ORFs): ORF1a, ORF1b, and ORF2. ORF1a and ORF1b encode the nonstructural proteins (NSPs), which are translated as a polypeptide and cleaved by cellular and viral proteins (19). ORF1a encodes a serine protease (11), a peptide (ORF1a/4) involved in virus localization and replication, and up to three other peptides of unknown function (8, 9). ORF1b encodes the viral RNA-dependent RNA polymerase (RdRp). Accumulation of the RdRp leads to production of the subgenomic RNA (sgRNA) from ORF2; this transcript encodes the single viral capsid protein (11, 27). The cellular factors regulating expression of these genes are currently unknown.

The mitogen-activated protein kinase (MAPK) pathways are global regulators of cellular responses to stress that transduce signals through subsequent phosphorylation events, culminating in phosphorylation of the terminal MAPK and altered cellular transcription profiles. Three major MAPK pathways, each named for its terminal MAPK, have been characterized to date: p38, Jnk, and extracellular signal-regulated kinase (ERK1/2 or MAPK 42/44) (14). The best-described ERK activation pathway is initiated by receptor tyrosine kinases that signal through the small G protein Ras. Activation of Ras leads to phosphorylation of Raf, which in turn phosphorylates MEK1/2, a dedicated dual-specificity kinase that controls ERK1/2 phosphorylation. Phosphorylated MEK1/2 activates ERK1/2 via phosphorylation on tyrosine and threonine residues (27). Activated ERK1/2 can translocate into the nucleus, where it activates transcription of numerous genes involved in cell survival, proliferation, and differentiation (17).

Many viruses exploit the ERK pathway for maximal viral replication. The regulation of cell cycle progression by ERK1/2 is an ideal target for many viruses. For example, enterovirus 71 prevents activation of the proapoptotic molecules caspase-9 and Bad by activating ERK1/2 (31). Conversely, the Ebola virus glycoprotein GP specifically inhibits ERK1/2, leading to increased cell toxicity and viral titers (32). ERK1/2 regulation of viral replication can also act at specific steps of the replication cycle, including entry, gene and protein expression, and assembly. Both human immunodeficiency virus type 1 and Borna disease virus require active ERK for entry (15, 23). Inhibition of ERK during coronavirus infection specifically decreases genomic and sgRNA production but has no effect on protein synthesis (4). In contrast, ERK activates adenovirus gene transactivators, modulating protein expression (28, 29) with little effect on RNA levels (28). Accumulation of the influenza virus surface protein hemagglutinin activates ERK1/2 late in infection (18, 24), in turn activating the viral nuclear export protein NS2/NEP and allowing transport of ribonucleoprotein complexes to the cytoplasm for packaging (18). ERK inhibition prevents viral assembly and decreases viral titers (24). Thus, the manipulation of the ERK pathway is not restricted to specific viral events or even viral classes but is a ubiquitous feature of viral infections.

Because of the myriad examples of ERK regulation of viral replication, we examined the role of this pathway during astrovirus infection. We demonstrated that HAstV activates ERK at early times during infection by a mechanism that is independent of viral replication. Inhibition of this pathway with MEK1/2 inhibitors PD98059 and U0126 significantly decreased viral replication regardless of cell type or viral serotype. Furthermore, ERK appears to be most important at early stages of the viral cycle; inhibition of ERK1/2 inhibited each step examined, including early and late protein expression, sgRNA and positive- and negative-strand RNA production, and virus production. Together, these data suggest an integral role for ERK1/2 in a postattachment step of the astrovirus replication cycle.

* Corresponding author. Mailing address: University of Wisconsin—Madison, Department of Medical Microbiology and Immunology, 1300 University Ave., 417 SMI, Madison, WI 53706. Phone: (608) 265-6462. Fax: (608) 262-8418. E-mail: slschul2@wisc.edu.

▽ Published ahead of print on 28 May 2008.

MATERIALS AND METHODS

Cell and virus propagation. The human intestinal adenocarcinoma cell line Caco-2 (catalog no. HTB-37) and mouse monoclonal 8E7 hybridoma (catalog no. HB-11945) were obtained from the American Type Culture Collection (ATCC, Manassas, VA) and were propagated as described previously (22). LLC-MK_2 (ATCC catalog no. CCL-2), 293 (ATCC catalog no. CRL-1573), and Vero (kind gift of David Watkins, University of Wisconsin—Madison) cells were propagated in minimal essential medium (MEM) containing 10% fetal bovine serum (Gemini Bio-Products, West Sacramento, CA). All cells were maintained under conditions of 37°C and 5% CO_2.

HAstV serotypes 1, 2, and 8 (HAstV-1, HAstV-2, and HAstV-8) (kind gifts of Stephen Monroe, Center for Disease Control and Prevention, Atlanta, GA, and Neel Krishna, Eastern Virginia Medical School) were propagated as described previously (30). Briefly, astrovirus at a multiplicity of infection (MOI) of 0.1 was pretreated with 5 μg/ml type IV porcine trypsin (Sigma-Aldrich, St. Louis, MO) in Dulbecco's modified Eagle's medium (DMEM) at 37°C for 15 min and added to serum-starved (1 h at 37°C) Caco-2 cells. Cells were incubated with rocking for 90 min at 37°C, after which the inoculum was removed and the cells were washed with DMEM. Maintenance medium containing 10 μg/ml porcine trypsin–DMEM was incubated on monolayers for 3 days at 37°C, with 5 μg/ml porcine trypsin added at day 2. Monolayers were subjected to one round of freeze-thaw treatment, and supernatants were collected by centrifugation (3,000 rpm for 10 min). Viral titers were obtained by serially diluting viral supernatants in DMEM–10 μg/ml trypsin and applying the mixture onto Caco-2 cells for 4 days at 37°C. After freezing and thawing, lysates were monitored by enzyme-linked immunosorbent assay (ELISA) as described below. The reciprocal of the last positive-well value corresponded to the titer of the virus; this number was used to determine subsequent MOIs. Viral stocks were aliquoted and stored at −80°C until use. Mock lysates containing trypsin were generated in the same manner, with omission of the viral inoculum.

Virus inactivation was conducted as described previously (22). Briefly, inocula were treated with 100 mJ/cm^2 UV by use of a UV cross-linker (Fisher Scientific, Norcross, GA). Inactivation was confirmed by passage of the UV-treated virus on Caco-2 cells followed by staining for HAstV-1 capsid protein as described below. Complete viral inactivation was defined as having occurred when a complete lack of capsid expression was seen.

Reagents and antibodies. All cell culture media were obtained from Mediatech (Fisher Scientific). The MEK1/2 inhibitors U0126 and PD98059, rabbit anti-ERK1/2, rabbit anti-phosphorylated ERK1/2 (pERK1/2), and the p38 inhibitor SB203580 were obtained from Promega (Madison, WI). Rabbit polyclonal antiserum against HAstV-1 was a kind gift of Dorsey Bass of Stanford University (1). The mouse monoclonal antiserum against HAstV-1 ORF1a/4 was a kind gift of Albert Bosch of the University of Barcelona, Barcelona, Spain (8). Monoclonal mouse anti-HAstV antibody 8E7 was purified from ascites fluid by use of a T-Gel purification system (Pierce, Rockford, IL) according to the manufacturer's instructions. Antibody concentrations were determined by bicinchoninic acid assay (Thermo Scientific, Rockford, IL).

HAstV ELISA. Fifty microliters of lysate from infected cells was incubated overnight at 4°C in D-lysine coated microtiter plates (Nunc, Rochester, NY). Wells were washed with phosphate-buffered saline (PBS) containing 0.1% Tween 20 (Fisher) and incubated with purified 8E7 antibody (~3 μg/ml) in detection buffer (PBS containing 25 mM Tris [pH 8.0] and 50% fetal bovine serum) for 1 h at 37°C. After being washed, wells were incubated with horseradish peroxidase (HRP)-conjugated goat anti-mouse antibody (Jackson Labs, Bar Harbor, ME) (diluted 1:5,000) in detection buffer for 1 h at 37°C, followed by incubation with HRP-colorimetric substrate (substrate reagent pack; R&D Systems, Minneapolis, MN) for 15 min at room temperature. The colorimetric reaction was stopped by the addition of 1 M H_2SO_4, and the difference between absorbance at 450 nm and absorbance at 605 nm (the relative absorbance) was determined. The ELISA was adapted from a protocol kindly provided by Stephen Monroe.

Time course of U0126 treatment. Caco-2 cells were mock infected or HAstV-1 (MOI of 5) infected as described above but were incubated at 4°C to synchronize infection. After a 1-h adsorption period, cells were washed, maintenance media (DMEM containing 10 μg/ml porcine trypsin) was added, and cells were shifted to 37°C. At −1, 0, 1, 2, 4, 8, or 12 h postinfection (hpi), U0126 was added to achieve a final 10 μM concentration for the remainder of the experiment. The infection was terminated at 24 hpi by freezing the monolayers at −80°C; the resulting lysates were examined for the presence of astrovirus by ELISA as described above.

Monitoring cell viability during ERK1/2 inhibition. Caco-2 cells were preincubated for 1 h at 37°C in the presence of dimethyl sulfoxide (DMSO) (0.1%), U0126 (10 μM), or PD9805 (50 μM). Cells were then mock infected or HAstV-1 (MOI of 5) infected in the presence of drug for 12 or 24 h at 37°C. Cell death was quantified by use of CellTiter 96 Aqueous One solution or Caspase-Glo 3/7 assay following the manufacturer's instructions (Promega, Madison, WI).

HAstV immunofluorescent microscopy. Caco-2 cells were mock infected or HAstV-1 (MOI 1) infected, and viral antigen was detected by immunofluorescence assay at various times pi. Briefly, monolayers fixed with ice-cold, absolute methanol for 15 min were blocked with 5% normal goat serum (NGS; Fisher Scientific) for 15 min at room temperature. ORF1a or capsid protein was detected by incubation with mouse anti-ORF1a/4 (diluted 1:1,000 in 1% NGS–PBS) or 8E7 supernatants (undiluted) for 90 min, followed by incubation with secondary antibody (Alexa 594-labeled goat anti-mouse, Invitrogen) (1:200) and DAPI (4′,6-diamidino-2-phenylindole; Invitrogen) (1:1,000) in 1% NGS–PBS for 1 h at room temperature. Coverslips were mounted with Prolong Gold (Invitrogen), and staining was visualized using an Axiovert 100 TV microscope (Zeiss, Germany). Data were analyzed with OpenLab software (Improvision, Lexington, MA).

ERK1/2 Western blotting. Caco-2 cells were mock infected or HAstV-1 (MOI 20) infected, or were treated with an equal amount of UV-inactivated virus (22), or stimulated with epidermal growth factor (EGF; BD Biosciences, Bedford, MA) (10 nM) for 10 min as a positive control (2). At the indicated times, monolayers were lysed in 300 μl of PBS containing 1% Triton X-100 (Fisher) and 1× protease inhibitor cocktail (Pierce) for 15 min at room temperature and centrifuged at 14,000 × *g* for 5 min at 4°C. Equal volumes of the soluble fraction were separated by sodium dodecyl sulfate-polyacrylamide gel electrophoresis (SDS-PAGE) (10%) under reducing conditions. Following transfer to nitrocellulose and a 1-h blocking in Tris-buffered saline containing 0.1% Tween 20 (TTBS; Fisher) and 1% bovine serum albumin (BSA; Sigma), membranes were probed with rabbit anti-pERK1/2 or anti-ERK1/2 (diluted 1:10,000 in TTBS containing 0.1% BSA) for 2 h at room temperature, followed by incubation with HRP-labeled goat anti-rabbit antibody (diluted 1:5,000 in 0.1% BSA–TTBS) for 1 h at room temperature. Signal was detected with SuperSignal West Pico chemiluminescent substrate (Pierce). To ensure equal loading, blots were quenched in 10% hydrogen peroxide (EMD, Darmstadt, Germany) for 30 min at room temperature and probed for total ERK1/2 as described above.

^{35}S-methionine protein labeling. Caco-2 cells were mock infected or HAstV-1 (MOI of 5) infected at 37°C in the presence of DMSO, U0126 (10 μM), or PD98059 (50 μM) after a 1-h preincubation with the corresponding drug. At 2 h prior to the 12- or 24-h time point, monolayers were washed twice with PBS and DMEM lacking L-glutamine, L-methionine, and L-cystine (MP Biomedicals, Solon, OH) and containing drug was added. After a 1-h starvation period, 100 μCi of ^{35}S-labeled L-methionine (ESPRE^{35}S^{35}S [^{35}S] protein labeling mix; PerkinElmer, Waltham, MA) was added to each well for incubation for 1 h at 37°C. Supernatants were removed and monolayers washed three times with PBS before cells were lysed in radioimmunoprecipitation assay buffer (0.2 ml) for 5 min on ice. Lysates were centrifuged (14,000 rpm for 5 min) and supernatants stored at −80°C until use. Equal volumes of lysate were separated by SDS-PAGE, dried, and exposed to a phosphoscreen. Images were developed using a Typhoon 8600 variable mode imager and processed with Typhoon scanner control software (Amersham, Piscataway, NJ).

HAstV-1 RT-PCR. Caco-2 cells were mock or HAstV-1 (MOI 5) infected in the presence or absence of U0126 (10 μM) as described above. At 4, 8, 12, or 24 hpi, RNA was extracted with TriZol reagent (Invitrogen) according to the manufacturer's instructions and 1 μg was subjected to semiquantitative reverse transcription-PCR (RT-PCR). RT reactions utilized Mon348 (positive strand), Mon344 (negative strand) (3), or GAPDH (glyceraldehyde-3-phosphate dehydrogenase) reverse primer (RNA control; 5′-AGTGATGGCATGGACTGTGG TCAT-3′) under the following conditions: 1× first-strand buffer, 10 mM dithiothreitol, 0.5 μM each deoxynucleoside triphosphate, 100 U Superscript II, 4 U RNAseOUT RNase inhibitor (Invitrogen), and 0.5 μM primer in a final volume of 20 μl. PCR mixtures were composed of the following: 1× FlexiTaq PCR buffer, 1.5 mM $MgCl_2$, 15 U GoTaq, 0.25 μM each deoxynucleoside triphosphate (Promega), 0.4 μM each forward and reverse primer, and 2 μl RT reaction mixture. Primer pairs included Mon340-Mon348 (positive strand) (3), Mon343-Mon344 (negative strand) (3), or GAPDH forward (5′-TCGACAGTCAGCCG CATCTTCTTT-3′) and reverse primers. Reactions occurred as follows: 1 cycle of 94°C for 3 min, 30 cycles of 94°C for 30 s, 59°C for 40 s, and 72°C for 30 s, and a final extension cycle of 72°C for 5 min. PCR products were separated on a 1% agarose gel and visualized on a Bio-Rad Gel Doc 1000 processor using multi-analyst software (Hercules, CA). Band intensities were compared using the NIH program Image J (http://rsb.info.nih.gov/ij/).

HAstV-1 genome analysis by Northern blotting. Caco-2 cells were mock infected or HAstV-1 infected (MOI of 10) in the presence or absence of U0126 (10

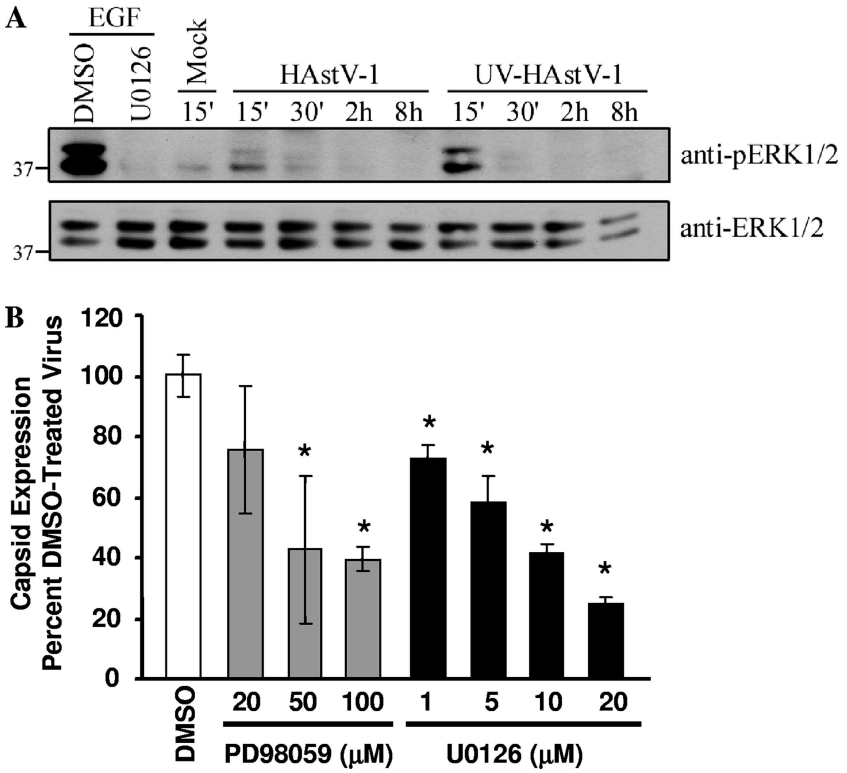

FIG. 1. ERK1/2 is involved in HAstV replication. (A) Caco-2 cells were treated with media alone, HAstV-1 (MOI of 20), or an equal amount of UV-inactivated HAstV-1 and cell lysates collected from 15 min pi to 8 hpi. As positive and negative controls, Caco-2 cells were preincubated with U0126 (10 μM) or vehicle control for 1 h and subsequently stimulated with EGF (10 nM). At the indicated times, cell lysates were separated by SDS-PAGE and the amounts of phosphorylated and total ERK1/2 evaluated by Western blotting. (B) Caco-2 cells were preincubated with increasing concentrations of U0126 or PD98059 or with vehicle control and then mock or HAstV-1 (MOI of 5) infected in the presence of drug. Viral production was measured by ELISA at 24 hpi. Data are representative of the results of at least two experiments. *, $P < 0.05$; error bars represent standard deviations.

μM). At 2, 4, 8, or 12 hpi, total RNA was isolated using TRIzol reagent and separated on a 0.7% agarose formaldehyde gel, transferred to a nylon filter, and UV cross-linked (Fisher Scientific). Blots were hybridized with ^{32}P-labeled probes specific to HAstV-1 ORF2 (nucleotides 4478 to 5027) and GAPDH for a loading control. The blots were washed extensively with increasing stringency (one washing with 2× SSC [1× SSC is 0.15 M NaCl plus 0.015 M sodium citrate]–0.1% SDS and two washings with 0.2× SSC–0.1% SDS at 15 min for each washing) and exposed to a phosphoscreen. Images were developed using a Typhoon 8600 variable mode imager and processed with Typhoon scanner control software (Amersham, Piscataway, NJ). Band intensities were quantified using Image J software.

Statistical analysis. All statistical analyses were examined by Student's *t* test, and statistical significance was represented by *P* values of less than 0.05.

RESULTS

HAstV-1 transiently activates ERK1/2. To determine whether HAstV infection activated ERK1/2, the phosphorylation status of ERK1/2 was monitored on Caco-2 cells at different times pi by Western blot analysis. For positive and negative controls, Caco-2 cells were preincubated with DMSO or the specific ERK inhibitor U0126 for 1 h and subsequently stimulated with EGF (10 nM) for 10 min, which led to phosphorylation of ERK1/2 (2). As expected, EGF treatment increased ERK1/2 phosphorylation, while U0126 treatment inhibited EGF-induced ERK1/2 phosphorylation (Fig. 1A). HAstV requires trypsin for successful replication in cell culture (21). Thus, all viral stocks contained traces of exogenous trypsin. Since trypsin can activate ERK1/2 (25), all mock lysates also contained an equal concentration of trypsin as a viral inoculum. In contrast to mock lysate-treated cell results, HAstV-1 infection led to increased ERK1/2 phosphorylation within 15 min pi that declined by 30 min pi, returning to background by 2 hpi. HAstV-1 had no effect on total ERK1/2 levels, which remained steady throughout the infection (Fig. 1A).

Based on the kinetics of ERK1/2 activation, we hypothesized that early events in viral infection were responsible for ERK1/2 activation. To examine this, Caco-2 cells were mock treated, HAstV-1 infected, or treated with equal amounts of UV-inactivated HAstV-1, which likely binds to cellular receptors but does not express new proteins (22). Monolayers treated with UV-inactivated HAstV-1 showed an activation profile similar to that seen with HAstV-1-treated monolayers, with increased ERK1/2 phosphorylation levels evident by 15 min pi that returned to background levels by 30 min pi (Fig. 1A). For unknown reasons, UV-inactivated virus appeared to activate ERK1/2 more efficiently than untreated virus. These results demonstrate that ERK1/2 activation occurs independently of viral replication. Since the mock-treatment mixtures contained equal amounts of trypsin, these results further suggest that increased ERK1/2 activation during HAstV-1 infection is independent of the presence of trypsin.

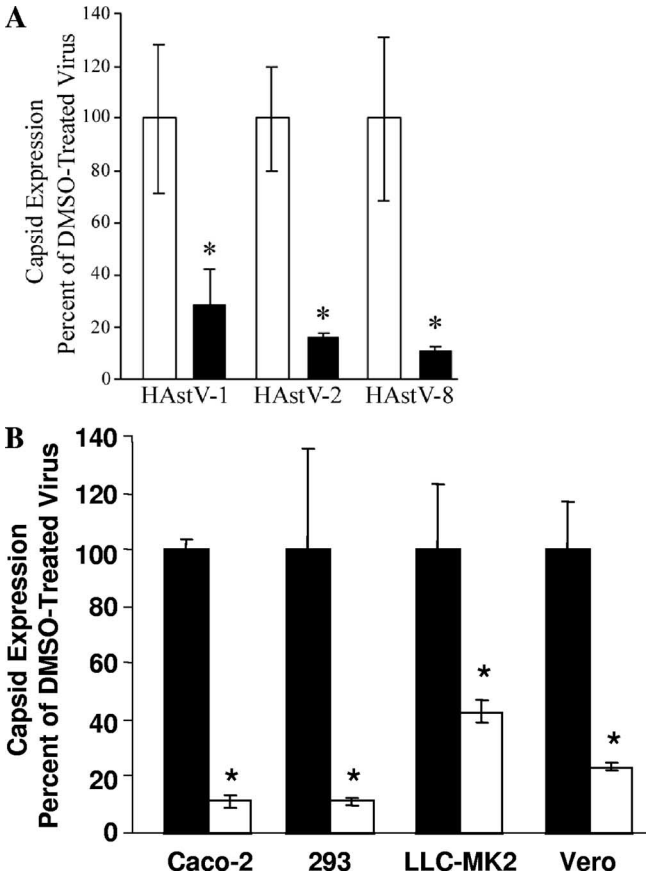

FIG. 2. ERK1/2 requirement is independent of HAstV serotype or cell type. (A) Caco-2 cells were preincubated with U0126 (10 μM; black bars) or DMSO (0.1%; white bars) and infected with HAstV-1, HAstV-2, or HAstV-8 (MOI of 5). Viral production at 24 hpi was monitored by ELISA. (B) Caco-2, LLC-MK2, Vero, and 293 cells were pretreated with U0126 (10 μM; white bars) or DMSO (0.1%; black bars) and infected with HAstV-2 (MOI of 5) in the presence of drug. Viral production was measured by ELISA at 24 hpi. ELISAs were performed in triplicate; data are representative of the results of at least three independent experiments. *, $P < 0.05$; error bars represent standard deviations.

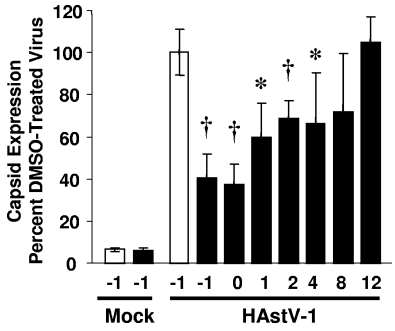

FIG. 3. ERK1/2 is required early in infection. Caco-2 cells were preincubated in the presence (10 μM; black bars) or absence (white bars) of U0126 and were mock or HAstV-1 (MOI of 5) infected at 4°C for 1 h prior to incubation at 37°C. At the indicated times, U0126 was added to achieve a final concentration of 10 μM. At 24 hpi, viral production was monitored by ELISA. Experiments were performed in triplicate; data are representative of the results of at least four independent experiments. *, $P < 0.01$; †, $P < 0.005$. Error bars represent standard deviations.

ERK1/2 regulates HAstV replication. To determine whether activated ERK is necessary for astrovirus replication, viral production was measured during ERK inhibition. Caco-2 cells were pretreated with the MEK1/2 inhibitor U0126 (1 to 20 μM) or PD98059 (20 to 100 μM) or with vehicle control (DMSO; 0.1%) and infected with HAstV-1, and viral production was measured by ELISA (Fig. 1B). U0126 is a highly potent inhibitor of ERK1/2 activation that acts by binding and inhibiting MEK1/2, the upstream activator of ERK1/2. PD98059 also inhibits ERK1/2 activation, albeit with about 2 logs less potency. PD98059 is thought to bind primarily to unphosphorylated MEK1/2, preventing its activation and subsequent ERK1/2 activation (6). U0126 decreased HAstV-1 antigen production at all concentrations tested ($P < 0.05$). A 50% inhibition was observed with 10 μM U0126 (Fig. 1B). PD98059 had no effect at a concentration of 20 μM but significantly decreased antigen production at concentrations at or above 50 μM. This response appeared to be specific to the ERK pathway, as pretreatment of cells with SB203580 (20 μM), an inhibitor of the p38 MAP kinase pathway, had no effect on viral antigen (data not shown).

To determine whether the ERK1/2 requirement was unique to HAstV-1, Caco-2 cells were preincubated with DMSO (0.1%) or U0126 (10 μM) for 1 h, followed by infection with HAstV-1, HAstV-2, or HAstV-8 (MOI of 5). Viral antigen levels were measured by ELISA. U0126 inhibition of ERK1/2 significantly decreased viral replication ($P < 0.01$) regardless of the serotype tested (Fig. 2A). These effects were also independent of the type of host cells, as U0126 (10 μM) treatment inhibited HAstV replication in Vero, LLC-MK2, and 293 cell lines ($P < 0.05$) (Fig. 2B), indicating that ERK1/2 universally regulates HAstV replication.

U0126 treatment blocks HAstV-1 replication at an early step in viral replication. To determine at which point ERK1/2 acted during the HAstV replication cycle, U0126 was added to Caco-2 cells at −1, 0, 1, 2, 4, 8, and 12 hpi. At 24 hpi, viral antigen levels were measured by ELISA (Fig. 3). Addition of U0126 1 h prior to or at the time of infection led to a 60% inhibition of viral titers compared to vehicle-treated control results ($P < 0.005$; Fig. 3). A 30% decrease in virus was observed when the inhibitor was added at between 1 and 4 hpi ($P < 0.05$). In contrast, no statistical differences in viral titers were observed when the inhibitor was added at 8 or 12 hpi ($P = 0.086$ or $P = 0.308$, respectively). These results suggest that ERK1/2 primarily acts at an early stage in infection.

Because ERK is known to modulate cell survival (31, 32) and because some serotypes of HAstV have been shown to increase cell death (7, 20), we first examined whether the decrease in viral expression was the result of increased death in the presence of ERK inhibition. Caco-2 cells pretreated with DMSO (0.1%), U0126 (10 μM), or PD98059 (50 μM) were mock or HAstV-1 infected, and viability was determined at 12 or 24 hpi by 3-(4,5-dimethylthiazol-2-yl)-5-(3-carboxymethoxyphenol)-2-(4-sulfophenyl)-2H-tetrazolium (MTS) assay (Fig. 4). At 12 hpi, the time at which we saw maximal effects on HAstV-1 replication, there was no difference in MTS levels between DMSO-treated mock-infected and HAstV-1-infected

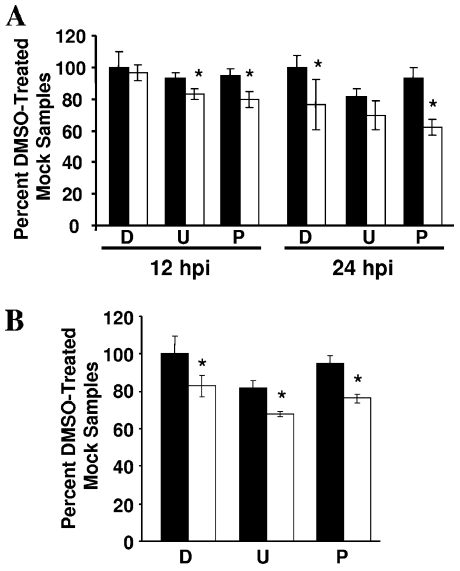

FIG. 4. ERK inhibition has a modest effect on cell death during HAstV infection. Caco-2 cells were preincubated in the presence of DMSO (0.1%), U0126 (10 μM), or PD9805 (50 μM). Cells were then mock or HAstV-1 (MOI of 5) infected in the presence of drug; viability was measured by an MTS assay of Caco-2 cells at 12 or 24 hpi (A) or of 293 cells at 12 hpi (B). Mock infection, black bars; HAstV-1 infection, white bars; D, DMSO; U, U0126; P, PD98059. *, $P < 0.05$ compared to drug control results; error bars represent standard deviations.

Caco-2 cells ($P = 0.297$) (Fig. 4A), with only a 20% decrease in death seen with ERK1/2 inhibitor-treated infected cells ($P < 0.05$). By 24 hpi, HAstV-1 infection alone resulted in a ~20% decrease in viability ($P < 0.05$) compared to the results seen with cells treated with DMSO. A similar decrease was noted with PD98059 compared to control results (Fig. 4A). Finally, cells treated with U0126 exhibited a ~20% decrease in viability regardless of the virus treatment (Fig. 4A). However, this minimal effect on viability was not accompanied by increased caspase activity, as measured by the Caspase-Glo 3/7 assay (data not shown). To evaluate whether these effects were specific to Caco-2 cells, viability in 293 cells was evaluated at 12 hpi (Fig. 4B). DMSO-treated cells infected with HAstV-1 showed a decrease (~20%; $P < 0.05$) in viability compared to mock-infected cells; a similar decrease was observed for PD98059-treated monolayers ($P < 0.05$). As in the Caco-2 cell results, treatment with U0126 alone decreased cellular viability by 20%. Addition of HAstV-1 led to a further ~15% decrease in viability over the results seen with drug alone (Fig. 4B). These results suggest that the effects of ERK inhibition were not due to a dramatic increase in cell death.

U0126 decreases HAstV-1 protein expression. To further evaluate the mechanism of ERK1/2 regulation of HAstV infection, we examined the effect of ERK inhibition on viral translation. Like all positive-sense RNA viruses, the HAstV genome is immediately translated upon release by use of the host cell translation machinery. Early HAstV-1 translation yields the NSPs, including RdRp. When sufficient quantities of these proteins have accumulated, transcription is initiated, eventually generating the capsid protein-encoding sgRNA, from which large quantities of capsid are translated. Thus, two phases in translation (early NSP versus late capsid protein expression) exist during infection. To determine whether either early or late protein expression was differentially affected during U0126 treatment, production of NSP1a/4 and capsid protein in the presence and absence of U0126 was monitored by immunofluorescent microscopy. Caco-2 cells were preincubated with DMSO (0.1%) or U0126 (10 μM) for 1 h and mock or HAstV-1 (MOI of 1) infected, and protein expression was monitored at 8 and 12 hpi. Expression of NSPs and structural proteins was evident at both time points regardless of treatment, but the intensity of staining per cell was markedly diminished in the presence of inhibitor (Fig. 5A), further confirming the ELISA results described above. The number of cells expressing viral antigen, as determined by capsid protein staining results, was also decreased during U0126 treatment (Fig. 5B). This was not the result of a nonspecific decrease in translation, as overall cellular protein levels remained similar, according to Coomassie staining results (Fig. 5C). Translation levels, as indicated by ^{35}S-labeled methionine incorporation, were also unaffected by treatment with U0126 or PD98059 (Fig. 5D). Thus, the effects on viral protein expression that were observed were likely due to the specific action of ERK during HAstV replication. Further, these data suggest that ERK regulation of the astrovirus replication cycle occurs at a stage prior to the considerable protein production evident at late time points.

HAstV-1 transcription is delayed during U0126 treatment. Two phases in transcription (negative- versus positive-strand expression) as well as two RNA entities (genomic versus subgenomic) can be distinguished during HAstV infection. To determine whether ERK1/2 inhibition prevented accumulation of genomic RNA or sgRNA, relative levels of both were examined by Northern blot analysis. Caco-2 cells were mock or HAstV-1 (MOI of 10) infected in the presence or absence of U0126 (10 μM). Total RNA was isolated, separated by electrophoresis, and transferred to a nylon membrane. The membrane was probed with labeled ORF2 fragments or human GAPDH as a loading control. Vehicle-control-treated cells produced detectable levels of both sgRNA and genomic RNA by 8 hpi. Levels increased through 12 hpi (Fig. 6A). Neither RNA entity was detected in U0126-treated cells until 12 hpi, and levels at this time were significantly decreased compared to control levels. Levels of genomic and sgRNA detected in U0126-treated samples were only about 45% of untreated levels. The sgRNA ratios between vehicle and U0126 treatment results throughout the time course did not drastically change, with sgRNA always present in excess. This is consistent with the results reported in the literature (21). The decreases in viral RNA levels during U0126 treatment were not due to nonspecific suppression of transcription, as GAPDH transcript levels in DMSO and U0126 samples remained similar (Fig. 6A and B). These observations suggest that ERK does not promote transcription of one RNA species over another; rather, there appears to be an overall decrease in RNA synthesis when ERK is inhibited.

This suppression could be due to inhibition of either positive- or negative-strand genome RNA synthesis. To evaluate this possibility, Caco-2 cells were mock or HAstV-1 (MOI of 5) infected in the presence of DMSO (0.1%) or U0126 (10 μM), total RNA was isolated at 4, 8, or 12 hpi, and 1 μg of RNA was

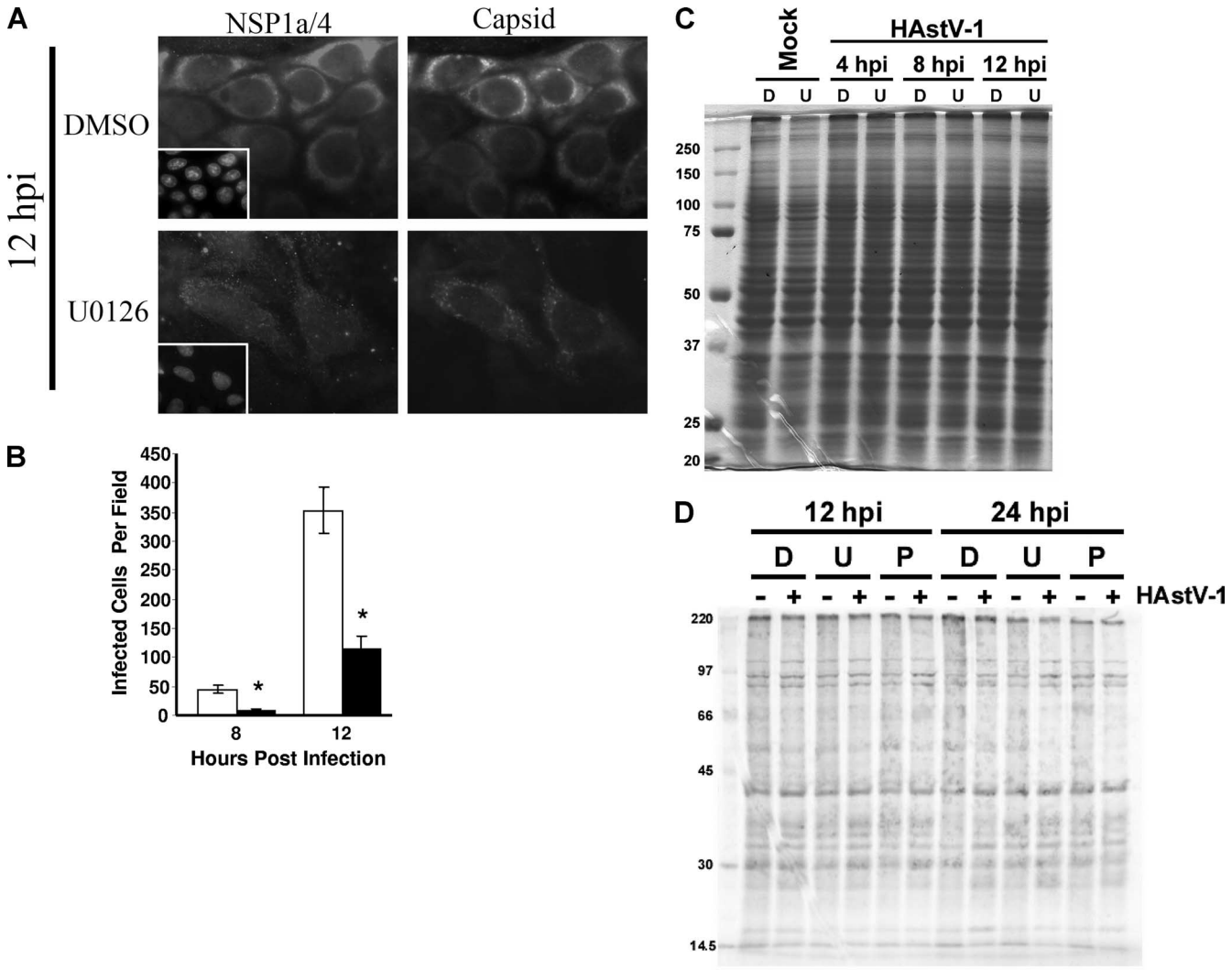

FIG. 5. U0126 delays HAstV-1 protein expression. Caco-2 cells were preincubated in the presence of U0126 (10 μM) or vehicle control (0.1%) for 1 h and then mock or HAstV-1 (MOI of 1) infected. (A) At the indicated times pi, monolayers were fixed, stained for nonstructural (early; NSP1a/4) or structural (late; 8E7) protein expression, and visualized by epifluorescent microscopy. Inserts present the results of DAPI staining. Data are representative of the results of at least three independent experiments. Magnification, ×40. (B) The number of cells expressing structural proteins per 10× field was quantified, and five to eight fields were counted per condition; the total number of cells per field was similar in all fields. (C) Caco-2 cells were preincubated with DMSO (0.1%) or U0126 (10 μM) for 1 h and mock or HAstV-1 (MOI 1) infected. At 4, 8, and 12 hpi, monolayers were lysed and equal volumes of lysate separated by SDS-PAGE. Proteins were visualized by Coomassie blue staining. (D) Caco-2 cells preincubated with drug were mock or HAstV-1 (MOI of 5) infected in the presence of DMSO, U0126 (10 μM), or PD98059 (50 μM). Protein synthesis was monitored by incubation with ^{35}S-labeled L-methionine (100 μCi) for 1 h. Cells were lysed in radioimmunoprecipitation assay buffer, and equal volumes of clarified lysate were separated by SDS-PAGE. D, DMSO; U, U0126; P, PD98059. *, $P < 0.05$; error bars represent standard deviations.

subjected to semiquantitative RT-PCR. Negative and positive RNA strands were detected during the RT step by using primers specific to the positive (Mon340)- or negative (Mon344)-sense genome; GAPDH levels were monitored to control for RNA loading. Again, suppression of viral RNA synthesis was observed (Fig. 6B). Vehicle-control-treated samples demonstrated detectable levels of negative-sense RNA by 8 hpi that increased through 12 hpi. Negative-strand RNA was not detectable until 12 hpi in U0126-treated samples and was present then at only about 42% of vehicle-treated levels. Similarly, levels of positive-strand RNA were decreased throughout U0126 treatment. At 8 and 12 hpi, the levels produced were only 50% and 70% of control levels, respectively. Positive-strand templates were detected prior to negative-strand templates, even though positive-strand synthesis occurs through a negative-strand RNA intermediate in positive-sense viruses. This is likely due to limitations in the sensitivity of the assay.

DISCUSSION

These studies demonstrate that activation of the MAP kinase ERK1/2 is important for optimal astrovirus replication in a manner that is independent of viral serotype and cell type. Our results suggest that ERK1/2 plays an important role dur-

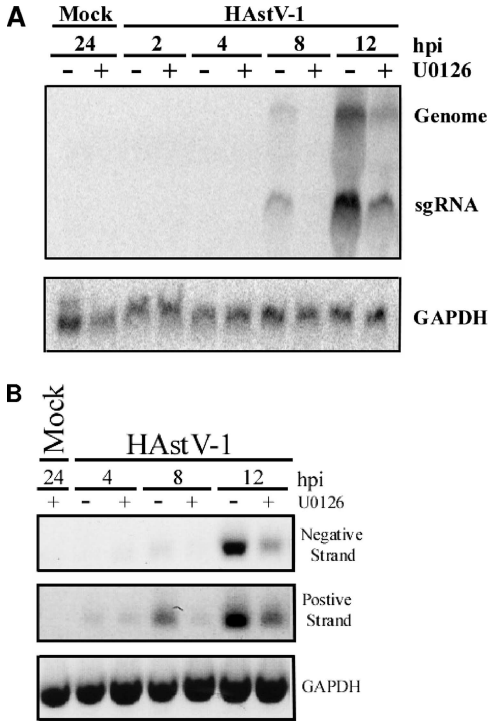

FIG. 6. U0126 decreases HAstV-1 RNA production. Caco-2 cells preincubated for 1 h in the presence of U0126 (10 μM) or vehicle control (0.1%) were mock or HAstV-1 (MOI of 10) infected, and RNAs were isolated at the indicated times pi. (A) Total RNA was separated on a formaldehyde agarose gel, transferred to a nylon membrane, and probed with a radiolabeled ORF2 or GAPDH probe. Genomic and sgRNA entities are indicated. (B) RNA (1 μg) was subjected to RT using specific positive (Mon344)- or negative (Mon340)-strand genome primers or reverse β-actin primers, followed by PCR with the corresponding primer pair. Reaction mixtures were separated on agarose gels. Data are representative of the results of at least three independent experiments.

ing an early stage in HAstV replication. ERK1/2 was transiently activated within 15 min of infection, and levels decreased by 30 min pi; by 2 hpi, activation levels returned to background. HAstV replication was inhibited upon pretreatment with the MEK1/2 inhibitors U0126 and PD98059. U0126 inhibited viral replication by ~40% when added up to 4 hpi, but subsequent addition had little effect, confirming that ERK is important at early steps of the viral cycle. Additionally, HAstV postattachment events evaluated were reduced in the presence of U0126: nonstructural and structural protein production was diminished and sgRNA transcript levels were decreased, as were negative and positive-strand genomic levels. Together, these data suggest an early requirement for ERK1/2 during HAstV infection.

Two major questions are generated by these data. First, how is ERK activated by astroviruses? The early activation kinetics of both infectious and UV-inactivated virus suggests that initial events in the viral life cycle lead to ERK activation. The rapid increase in ERK1/2 phosphorylation suggests that activation may be mediated by receptors. The best-described ERK1/2 activation pathway initiates with receptor tyrosine kinases, although substrate binding to ion channels can also activate ERK (27). Determination of the viral receptor should yield significant insight into whether or not the receptor participates directly in ERK activation. An alternative possibility is that ERK is activated by the viral entry process. Astroviruses enter cells by receptor-mediated endocytosis (5). Studies of other systems have demonstrated that dynamin activity, which regulates membrane invagination during endocytosis, can activate ERK (13). Additionally, ERK signal cascade components have been localized to endosomes and may be activated when a substrate (such as a virus) is trafficked through the endosomal pathway (26). The likelihood of these explanations depends on how quickly the virus enters the cells, data which are currently unknown for astroviruses. Studies are under way to investigate these possibilities.

The second question concerns the function of activated ERK during astrovirus infection. ERK activation may regulate viral replication directly or indirectly. Positive-sense RNA virus RdRps are increasingly recognized as being phosphorylated by host proteins (10). ERK is believed to phosphorylate and activate the coxsackievirus B3 RdRp (16); a similar phosphorylation event could be necessary to activate or stabilize the HAstV RdRp. Putative ERK binding sites on the HAstV-1 NSPs have been predicted by in silico screening (data not shown), offering the tempting possibility that ERK may phosphorylate the RdRp. This hypothesis could explain the HAstV suppression observed during ERK1/2 inhibition. Reduced levels of NSPs, particularly RdRp, would yield less RNA, as has been observed during U0126 treatment. Alternatively, the influence of ERK1/2 could be indirect. In several systems, ERK1/2 activation leads to the activation of transcription factors important in viral replication. In these cases, inhibition of ERK limits but often does not eliminate viral replication, suggesting that this pathway is only one of several pathways important for normal viral replication. This is reminiscent of what is observed during astrovirus infection, as ERK inhibition decreases but does not eliminate viral replication.

For all parameters, U0126-treated sample expression was delayed and/or repressed until 12 hpi in comparison to control-treated sample results. For example, expression of both genomic and sgRNA in control-treated cells is detectable at 8 hpi by Northern blot analysis. Levels increased through 12 hpi. In contrast, U0126-treated samples did not produce detectable levels of either RNA species until 12 hpi, even when the blot was overexposed (data not shown). The amount of RNA produced was ~45% of vehicle-treated RNA levels at 12 hpi. This trend was also observed when measuring negative- and positive-strand synthesis by RT-PCR and protein expression by immunofluorescence assay. The reasons behind this temporal delay are currently unknown.

Although the exact mechanism by which ERK1/2 regulates astrovirus infection is currently unknown, it is unlikely to be the result of increased cell death rates. There was no increase in death rates at 12 hpi for Caco-2 cells; by 24 hpi, a modest increase was noted. In the presence of ERK1/2 inhibitors, we saw a ~20% decrease in viability, which seems unlikely to explain the drastic decrease in virus replication. Activation of caspases was not observed in this time frame (data not shown). Further, no increase in cell death rates has been observed by our laboratory during astrovirus infection in vitro (22) or in vivo (12). These results do not necessarily contradict earlier studies into HAstV-induced cell death rates. Previous studies

demonstrated that HAstV-4 (7) and HAstV-8 (20) induced cell death; however, this occurred at later times pi (beyond 24 hpi). We clearly demonstrate that ERK1/2 inhibition affects numerous stages of the viral replication cycle by 12 hpi. Thus, while we are not excluding the possibility of increased cell death, it appears to play a role later in infection and is unlikely to be the means by which ERK1/2 is regulating early viral events.

In conclusion, we have demonstrated that HAstV infection activates ERK1/2 early in infection in a manner independent of viral replication and viral serotype. The mechanism by which ERK activity regulates viral processes during infection remains unclear; however, inhibition of ERK significantly delays nonstructural and structural viral protein expression as well as production of sgRNA and genomic RNA. Further investigations into the mechanisms of astrovirus activation of ERK and ERK regulation of viral processing are the focus of continuing studies by our laboratory.

ACKNOWLEDGMENTS

We thank Charles Czuprynski for providing the original inhibitor panel, Albert Bosch for anti-ORF1a/4 antibody, and Stephen Monroe and Neel Krishna for HAstV viral stocks and antibody. Thanks also to Jay Bangs for use of his microscope and Kevin Schwarz, Laura Knoll, and Peg Rooney for technical assistance. Thanks to Rose Szabady and members of the Schultz-Cherry laboratory for discussions and critical reviews of the manuscript.

L.A.M. was funded by an AGA Student Research Fellowship Award and a Microbial Pathogenesis and Host Responses training grant (NIH T32 A10055397). S.S.-C. was supported by start-up funds from the University of Wisconsin—Madison.

REFERENCES

1. **Bass, D. M., and U. Upadhyayula.** 1997. Characterization of human serotype 1 astrovirus-neutralizing epitopes. J. Virol. **71:**8666–8671.
2. **Basuroy, S., A. Seth, B. Elias, A. P. Naren, and R. Rao.** 2006. MAPK interacts with occludin and mediates EGF-induced prevention of tight junction disruption by hydrogen peroxide. Biochem. J. **393**(Pt. 1)**:**69–77.
3. **Belliot, G., H. Laveran, and S. S. Monroe.** 1997. Detection and genetic differentiation of human astroviruses: phylogenetic grouping varies by coding region. Arch. Virol. **142:**1323–1334.
4. **Cai, Y., Y. Liu, and X. Zhang.** 2007. Suppression of coronavirus replication by inhibition of the MEK signaling pathway. J. Virol. **81:**446–456.
5. **Donelli, G., F. Superti, A. Tinari, and M. L. Marziano.** 1992. Mechanism of astrovirus entry into Graham 293 cells. J. Med. Virol. **38:**271–277.
6. **Favata, M. F., K. Y. Horiuchi, E. J. Manos, A. J. Daulerio, D. A. Stradley, W. S. Feeser, D. E. Van Dyk, W. J. Pitts, R. A. Earl, F. Hobbs, R. A. Copeland, R. L. Magolda, P. A. Scherle, and J. M. Trzaskos.** 1998. Identification of a novel inhibitor of mitogen-activated protein kinase kinase. J. Biol. Chem. **273:**18623–18632.
7. **Guix, S., A. Bosch, E. Ribes, L. Dora Martinez, and R. M. Pinto.** 2004. Apoptosis in astrovirus-infected CaCo-2 cells. Virology **319:**249–261.
8. **Guix, S., S. Caballero, A. Bosch, and R. M. Pinto.** 2004. C-terminal nsP1a protein of human astrovirus colocalizes with the endoplasmic reticulum and viral RNA. J. Virol. **78:**13627–13636.
9. **Guix, S., S. Caballero, A. Bosch, and R. M. Pinto.** 2005. Human astrovirus C-terminal nsP1a protein is involved in RNA replication. Virology **333:**124–131.
10. **Jakubiec, A., and I. Jupin.** 2007. Regulation of positive-strand RNA virus replication: the emerging role of phosphorylation. Virus Res. **129:**73–79.
11. **Jiang, B., S. S. Monroe, E. V. Koonin, S. E. Stine, and R. I. Glass.** 1993. RNA sequence of astrovirus: distinctive genomic organization and a putative retrovirus-like ribosomal frameshifting signal that directs the viral replicase synthesis. Proc. Natl. Acad. Sci. USA **90:**10539–10543.
12. **Koci, M. D., L. A. Moser, L. A. Kelley, D. Larsen, C. C. Brown, and S. Schultz-Cherry.** 2003. Astrovirus induces diarrhea in the absence of inflammation and cell death. J. Virol. **77:**11798–11808.
13. **Kranenburg, O., I. Verlaan, and W. H. Moolenaar.** 1999. Dynamin is required for the activation of mitogen-activated protein (MAP) kinase by MAP kinase kinase. J. Biol. Chem. **274:**35301–35304.
14. **Lewis, T. S., P. S. Shapiro, and N. G. Ahn.** 1998. Signal transduction through MAP kinase cascades. Adv. Cancer Res. **74:**49–139.
15. **Liu, N. Q., A. S. Lossinsky, W. Popik, X. Li, C. Gujuluva, B. Kriederman, J. Roberts, T. Pushkarsky, M. Bukrinsky, M. Witte, M. Weinand, and M. Fiala.** 2002. Human immunodeficiency virus type 1 enters brain microvascular endothelia by macropinocytosis dependent on lipid rafts and the mitogen-activated protein kinase signaling pathway. J. Virol. **76:**6689–6700.
16. **Luo, H., B. Yanagawa, J. Zhang, Z. Luo, M. Zhang, M. Esfandiarei, C. Carthy, J. E. Wilson, D. Yang, and B. M. McManus.** 2002. Coxsackievirus B3 replication is reduced by inhibition of the extracellular signal-regulated kinase (ERK) signaling pathway. J. Virol. **76:**3365–3373.
17. **Luttrell, L. M.** 2003. "Location, location, location": activation and targeting of MAP kinases by G protein-coupled receptors. J. Mol. Endocrinol. **30:**117–126.
18. **Marjuki, H., M. I. Alam, C. Ehrhardt, R. Wagner, O. Planz, H. D. Klenk, S. Ludwig, and S. Pleschka.** 2006. Membrane accumulation of influenza A virus hemagglutinin triggers nuclear export of the viral genome via protein kinase Cα-mediated activation of ERK signaling. J. Biol. Chem. **281:**16707–16715.
19. **Matsui, S. M., and H. B. Greenberg.** 1996. Astroviruses, p. 811–824. *In* B. N. Fields, D. M. Knipe, and P. M. Howley (ed.), Fields virology, 3rd ed. Lippincott-Raven Publishers, Philadelphia, PA.
20. **Méndez, E., E. Salas-Ocampo, and C. F. Arias.** 2004. Caspases mediate processing of the capsid precursor and cell release of human astroviruses. J. Virol. **78:**8601–8608.
21. **Monroe, S. S., S. E. Stine, L. Gorelkin, J. E. Herrmann, N. R. Blacklow, and R. I. Glass.** 1991. Temporal synthesis of proteins and RNAs during human astrovirus infection of cultured cells. J. Virol. **65:**641–648.
22. **Moser, L. A., M. Carter, and S. Schultz-Cherry.** 2007. Astrovirus increases epithelial barrier permeability independently of viral replication. J. Virol. **81:**11937–11945.
23. **Planz, O., S. Pleschka, and S. Ludwig.** 2001. MEK-specific inhibitor U0126 blocks spread of Borna disease virus in cultured cells. J. Virol. **75:**4871–4877.
24. **Pleschka, S., T. Wolff, C. Ehrhardt, G. Hobom, O. Planz, U. R. Rapp, and S. Ludwig.** 2001. Influenza virus propagation is impaired by inhibition of the Raf/MEK/ERK signalling cascade. Nat. Cell Biol. **3:**301–305.
25. **Riteau, B., C. de Vaureix, and F. Lefevre.** 2006. Trypsin increases pseudorabies virus production through activation of the ERK signalling pathway. J. Gen. Virol. **87**(Pt. 5)**:**1109–1112.
26. **Robertson, S. E., S. R. Setty, A. Sitaram, M. S. Marks, R. E. Lewis, and M. M. Chou.** 2006. Extracellular signal-regulated kinase regulates clathrin-independent endosomal trafficking. Mol. Biol. Cell **17:**645–657.
27. **Rubinfeld, H., and R. Seger.** 2005. The ERK cascade: a prototype of MAPK signaling. Mol. Biotechnol. **31:**151–174.
28. **Schümann, M., and M. Dobbelstein.** 2006. Adenovirus-induced extracellular signal-regulated kinase phosphorylation during the late phase of infection enhances viral protein levels and virus progeny. Cancer Res. **66:**1282–1288.
29. **Whalen, S. G., R. C. Marcellus, A. Whalen, N. G. Ahn, R. P. Ricciardi, and P. E. Branton.** 1997. Phosphorylation within the transactivation domain of adenovirus E1A protein by mitogen-activated protein kinase regulates expression of early region 4. J. Virol. **71:**3545–3553.
30. **Willcocks, M. M., M. J. Carter, F. R. Laidler, and C. R. Madeley.** 1990. Growth and characterisation of human faecal astrovirus in a continuous cell line. Arch. Virol. **113:**73–81.
31. **Wong, W. R., Y. Y. Chen, S. M. Yang, Y. L. Chen, and J. T. Horng.** 2005. Phosphorylation of PI3K/Akt and MAPK/ERK in an early entry step of enterovirus 71. Life Sci. **78:**82–90.
32. **Zampieri, C. A., J. F. Fortin, G. P. Nolan, and G. J. Nabel.** 2007. The ERK mitogen-activated protein kinase pathway contributes to Ebola virus glycoprotein-induced cytotoxicity. J. Virol. **81:**1230–1240.